Journal of Colloid and Interface Science 621 (2022) 431–439

Contents lists available at ScienceDirect

Journal of Colloid and Interface Science

journal homepage: www.elsevier.com/locate/jcis

Theory of oil fouling for microfiltration and ultrafiltration membranes in produced water treatment

Ettore Virga [a,b], Robert W. Field [c], P.M. Biesheuvel [b], Wiebe M. de Vos [a,*]

[a] Membrane Science and Technology, University of Twente, Drienerlolaan 5, 7522 NB Enschede, the Netherlands
[b] Wetsus, European Centre of Excellence for Sustainable Water Technology, Oostergoweg 9, 8911 MA Leeuwarden, the Netherlands
[c] University of Oxford, Department of Engineering Science, Parks Road, Oxford OX1 3PJ, UK

GRAPHICAL ABSTRACT

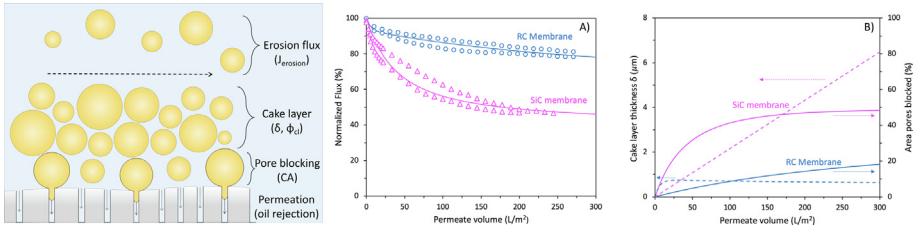

ARTICLE INFO

Article history:
Received 21 January 2022
Revised 5 April 2022
Accepted 6 April 2022
Available online 18 April 2022

Keywords:
Produced water treatment
Membrane fouling
O/W emulsion
Fouling modelling

ABSTRACT

Due to the complexity of oil-in-water emulsions, the existing literature is still missing a mathematical tool that can describe membrane fouling in a fully quantitative manner on the basis of relevant fouling mechanisms.

Hypothesis: In this work, a quantitative model that successfully describes cake layer formation and pore blocking is presented. We propose that the degree of pore blocking is determined by the membrane contact angle and the resulting surface coverage, while the cake layer is described by a mass balance and a cake erosion flux.

Validation: The model is validated by comparison to experimental data from previous works (Dickhout et al. 2019; Virga et al., 2020) where membrane type, surfactant type and salinity were varied. Most input parameters could be directly taken from the experimental conditions, while four fitting parameters were required.

Findings: The experimental data can be well described by the model which was developed to provide insight into the dominant fouling mechanisms. Moreover, where existing models usually assume that pore blocking precedes cake layer formation, here we find that cake layer formation can start and occur while the degree of pore blocking is still increasing, in line with the more dynamic nature of oil droplets filtration. These new conceptual advances in the field of colloid and interface science open up new pathways for membrane fouling understanding, prevention and control.

1. Introduction

One of the most difficult technological challenges in the field of environmental technology, with huge environmental impact, is the treatment and reuse of produced water (PW), a massive stream of oily wastewater originated from Oil & Gas (O&G) extraction. Glob-

* Corresponding author.
E-mail address: w.m.devos@utwente.nl (W.M. de Vos).

https://doi.org/10.1016/j.jcis.2022.04.039
0021-9797/

ally, the ratio between the volume of water used per volume of oil extracted is expected to reach a number beyond 10 by 2025 due to the ageing of the wells [3], with over 30 billion of m^3 of produced water in 2020 alone [4]. Given the massive worldwide production of PW, the need for better PW treatment is of significant importance, especially in areas where water is already scarce and PW, if well treated, could be immediately reused in industry or agriculture [5].

Membranes have been demonstrated to successfully tackle the challenging separation of oil-in-water (O/W) emulsions like PW, even when the presence of small oil droplets (<10μm in diameter) makes treatment by other technologies ineffective [6]. Especially microfiltration (MF) and ultrafiltration (UF) membranes have been applied for the treatment of PW, as these membranes can potentially remove a great part of the oil at high water permeability [7–11].

However, the broader use of pressure-driven membranes for produced water treatment is still limited by membrane fouling [6,12,13] and surfactants alone can cause significant fouling [14,15]. For MF and UF, fouling during PW treatment is mainly due to the deposition of oil droplets at the membrane interface, and it is often responsible for substantial flux declines and increases in operating costs. Normally, membrane fouling mechanisms can be grouped into four main categories (complete pore blocking, standard blocking, intermediate blocking, and cake layer formation [6,8]) that will be later discussed in detail. Understanding and quantifying the mechanisms that lead to oil fouling in PW treatment, including the role of the chemistry of the emulsion and the membrane surface chemistry and pore size, are crucial for designing better membranes and to make more effective use of chemicals and process conditions to mitigate membrane fouling.

Many studies have investigated and tried to model fouling by O/W emulsions, such as PW, for MF and UF membranes. By far the largest part of these studies are based on Hermia's fouling model [16] (which was just for dead-end filtration) and related extensions made to Hermia's model to allow for crossflow [17]. For example, Koltuniewicz et al. studied, for a variety of membranes, in both dead-end and crossflow experiments, the effect of pressure and crossflow velocity on flux decline [18]. Pan et al. prepared a tubular coal-based carbon MF membrane for with uniform pore structure and narrow pore size distribution and then modeled fouling with Hermia's model [19]. Salahi et al. employed the model to study the fouling mechanism of the filtration processes of different polymeric membranes [20]. Abbasi et al. synthesized mullite ceramic MF membranes for treatment of oily wastewaters and investigated their fouling mechanisms using the adapted Hermia model introduced by Field et al. [17,21]. Masoudnia et al. tested and also modeled fouling for polyvinylidene fluoride membranes under various operating conditions [22] by using Hermia's original model. However, while Hermia's model is an excellent phenomenological model, it is only a qualitative tool as it does not predict fouling a priori but it is limited by being based on pure fitting as is the recent approach of Wu [23]. Moreover, an underlying assumption is that the fouling agents act as solids, while emulsion droplets are well known to be able to deform and coalesce.

Recently, other modeling studies focused mainly on oil droplet-membrane interactions. Salama et al. identified and modeled two basic mechanisms to explain fouling during oily wastewater filtration, i.e. fouling due to pinning of oil droplets and coalescence of oil droplets [24]. Tanudjaja et al. used classical models for colloid interactions, to quantify the foulant-membrane and foulant-foulant interactions [25]. Galvagno et al. have shown the existence of different equilibria regions (stable, bistable and unstable) which indicate if an oil droplet will deposit or not on a membrane surface [26]. Darvishzadeh et al. estimated analytically the critical permeation pressure from a force balance model that involves the drag force from the flow around the droplet and surface tension forces as well as the pressure variation inside the pore [27]. However, what is still missing in the existing literature is a tool that gives specific insights on the fouling mechanisms based on measurable emulsion (feed) properties (e.g. oil droplet size, oil permeation, oil-membrane contact angle, etc.). Such a model would benefit PW treatment with membranes by offering more insight into the membrane fouling, thereby indicating quantitative solutions to mitigate fouling.

In this work, we present a quantitative but still simple model which predicts flux decline over time in MF and UF systems based on feed and membrane properties. By modelling pore blocking as directly connected to the membrane/oil contact angle and the cake layer via a mass balance limited by an erosion flux, as shown in Fig. 1, one obtains insights into how membrane fouling occurs. The model is validated by comparison to experimental data for varying membrane type, surfactant type and salinity of the feed stream. We find good agreement between the model and the experimental data. Moreover, where existing models usually predict that pore blocking precedes cake layer formation, here we find that these mechanisms are expected to occur simultaneously, due to the dynamic nature of the oil droplets.

2. Materials and methods

2.1. Theory

2.1.1. Fouling mechanisms

Membrane fouling in PW treatment for MF and UF usually refers to the deposition of substances on the membrane surface, such as oil droplets or solid particles. This causes a flux decline of the water phase permeating through the membrane, which indirectly allows us to determine the extent of fouling.

Fouling mechanisms are traditionally categorised into four different processes that can take place: complete pore blocking, standard pore blocking, intermediate blocking and cake layer filtration. In complete pore blocking, the pore is blocked by a large particle and no more water can pass through. In standard blocking, small particles coat the inside of the pores, narrowing the channels and thus lowering the flux. In intermediate blocking, particles build up on top of the membrane surface, narrowing the pore entrances. The fourth process is cake filtration which refers to the formation of a layer of particles on the surface of the membrane. This layer is not impermeable, but adds an additional resistance and sometimes also additional selectivity. Dickhout et al. proposed an additional fifth fouling mechanism which might play a role in membrane fouling by PW [8]. In this process, oil droplets are coalescing on the membrane surface, forming a patchy continuous oil layer on the surface.

As the oil droplets in PW are much larger than the membrane pores, in our model we describe fouling only in terms of complete pore blocking and cake layer filtration (processes 1 and 4 mentioned above). Fouling due to coalescence and formation of a continuous oil layer can be modeled as a limiting situation when the cake layer porosity is extremely low. The modelling of the combination of complete pore blocking and cake layer filtration is carefully described in the following sections.

2.1.2. Model hypotheses

In this work, a key assumption is to assume the cake layer porosity as constant, or in other words, of the volume fraction of the droplets that constitute the cake. We assume that in the cake layer we have a fixed volume fraction, which we call ϕ_{CL}, that is relatively constant across the cake. Oil droplets could also coalesce and/or be pushed through the pores of the membrane. These

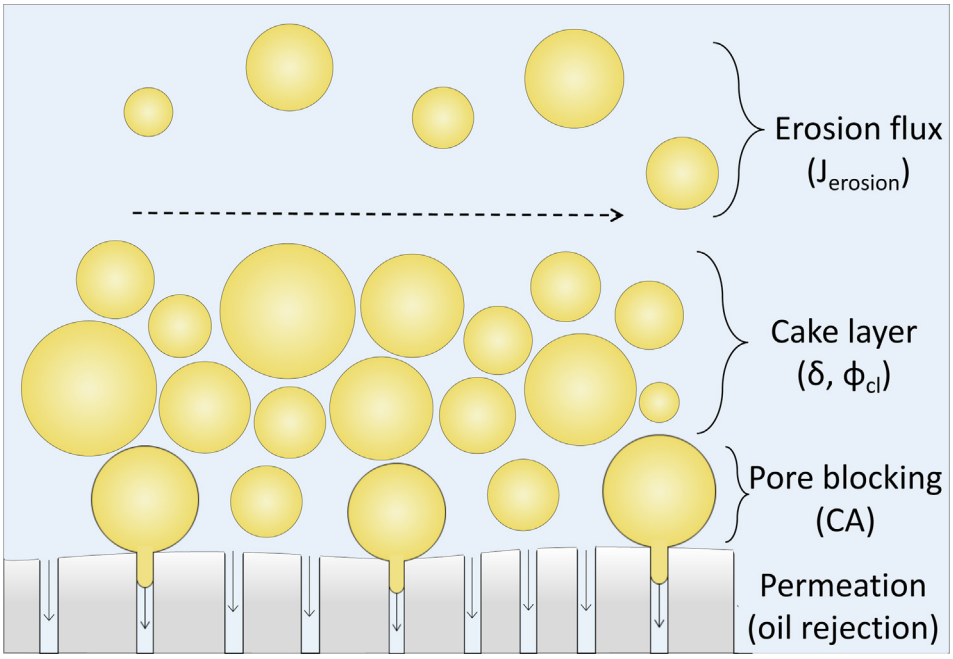

Fig. 1. Illustration of membrane fouling by oil droplets and main parameters of cake layer, pore blocking, and erosion flux, i.e. erosion flux $J_{erosion}$, cake layer thickness δ, volume fraction of oil in the cake layer ϕ_{cl}, oil-membrane contact angle CA, and oil rejection by the membrane.

effects related to deformation of the droplets can be significant, especially for relatively large droplets with low surface tensions. If these phenomena do occur, we assume that such deformations take place during the first minutes of filtration. This allows us to assume a cake layer porosity that is constant over time and across the cake.

2.1.3. Equation for complete pore blocking

In this section we derive, to the best of our knowledge, a new formula to describe complete pore blocking by oil droplets, where we correlate the number of blocked pores directly to a measurable physical parameter, the oil-membrane (in water) contact angle.

Herein the total resistance is taken to be the sum of the membrane resistance (which includes pore blocking) and the cake resistance which is a resistance in series. Due to complete pore blocking, the resistance of the membrane, R_m, will increase with the permeate volume as more and more droplets are transported to the membrane surface. However, we can expect that an oil droplet in contact with the membrane surface will cover more or less pores depending on its affinity for the membrane material. This affinity results in a specific oil-membrane contact angle, CA, in water. For an oil droplet in contact with the membrane surface, the contact area A_{cont} can be expressed by

$$A_{cont} = \pi\left(\frac{d_p}{2}\sin(CA)\right)^2. \quad (1)$$

If we consider the pores of the membrane fully blocked for CA < 90° (high affinity between oil and membrane) we can then write the the area of the membrane A_{memb} covered because of oil adhesion A_{cov} as

$$A_{cov} = \sin^2(CA)\cdot A_{memb}. \quad (2)$$

At steady state, when all the oil droplets have been transported to the membrane surface and there is no room for more droplets on top of the same surface, the membrane resistance due to pore blocking will only depend on the contact angle, with $R_m = \frac{R_0}{1-\sin^2(CA)}$. A high contact angle allows for more membrane pores to be open. A high affinity between oil droplets and membrane surface translates into lower contact angles and, as droplets spread more over the membrane surface, more pores will be "blocked".

With this in mind, and assuming that the membrane resistance goes exponentially to its steady state value, we can write how the membrane resistance R_m changes with pore blocking by

$$R_m = \frac{R_0}{1-\sin^2(CA)}\cdot\left(1-\sin^2(CA)\cdot e^{-\tau_{pb}v}\right) \quad (3)$$

where R_0 (m^{-1}) is the resistance of the clean membrane, CA is the oil contact angle measured for an oil droplet in contact with the membrane surface in water, v (L) is the permeate volume, and τ_{pb} (L^{-1}) a model parameter which indicates how fast the droplets adhere to the membrane surface. The equation is independent of the droplet size.

2.1.4. Equations for Cake Layer Filtration

In this section, we derive a new model for the dynamics of cake layer growth in crossflow filtration relevant for MF/UF of oily wastewaters, such as PW. The new model is here derived for the erosion rate $J_{erosion}$ of a cake layer, i.e. rate of re-entrainment of oil into the crossflow from the cake layer per unit membrane area. We derive a result that shows how $J_{erosion}$ depends on the thickness δ and water flow rate J_w through the membrane at any moment in time. Field et al. previously modified Hermia's expressions to account for a removal term [17,28] in the calculation of the flux decline. However, we are not aware of an expression for erosion flux similar to the one we derive that can be directly used in a cake layer mass balance and which thereby allows for a self-consistent calculation of the growth of the cake layer and the resulting decline of water flux.

The expression we will derive for $J_{erosion}$ is part of a total model that has two additional equations. These two additional equations are as follows. The first one is an expression for the flow rate J_w versus membrane resistance R_m, cake layer permeability k, and thickness δ

$$J_w = \frac{\Delta P}{\mu(R_m + k\delta)} \tag{4}$$

with ΔP (Pa) the pressure applied across the membrane, $k = \frac{150\delta\phi_{CL}^2}{D_p^2(1-\phi_{CL})^3}$ (m^{-1}) is a permeability parameter whose value can be calculated from the Kozeny-Carman equation, where ϕ_{cl} the volume fraction of oil in the cake layer, and D_p (m) is the average diameter of the oil droplets. The second equation is a mass balance for the total amount of material in the cake (e.g. oil droplets)

$$\phi_{cl}\frac{d\delta}{dt} = J_w \cdot (\phi_\infty - \phi_{perm}) - J_{erosion}, \tag{5}$$

where ϕ_{cl}, ϕ_∞ and ϕ_{perm} are the volume fractions of oil in the cake layer, in the bulk of the feed, and in the permeate, respectively. For a constant cake layer volume fraction, ϕ_{cl}, this mass balance can be expressed as a time dependence of thickness. This mass balance includes the erosion rate and also advective 'addition' of fresh material into the cake, and 'leakage' of droplets from cake through the membrane to the permeate side.

Though this full model consists of three equations, they can be combined into one long ordinary differential equation (ODE), but for numerical modeling (e.g., using commercial spreadsheet softwares) this is not necessary, and the several required equations can be solved 'side by side'. It is useful to rewrite Eq. (5) such that it does not explicitly depend on time, t, but that it depends on the permeated volume, v. Differentiating with respect to the permeate volume v and taking into account that $\frac{dv}{dt} = J_w \cdot A_m$, where A_m (m^2) is the membrane area, we can rewrite Eq. (5) to

$$A_m\phi_{cl}\frac{d\delta}{dv} = \phi_\infty - \phi_{perm} - \frac{J_{erosion}}{J_w}. \tag{6}$$

In solving this model, we can 'step through time' using an explicit or implicit (Euler) scheme. Interestingly, to arrive at an analytical equation for water flow as function of time t or volume v, actually quite stringent simplifications must be made, and in this paper we will not discuss that research direction. Instead we only present results of the full numerical analysis based on Eqs. (3), (4), and (6). All parameter settings are described in Supporting Material, Table S1. We solve the new model dynamically, for a one-dimensional geometry, for a given applied pressure. But in future work, also other simulations are possible where the setpoint for transmembrane pressure is changed (e.g., stepwise), and we follow in time the change of cake layer thickness and flow rate as they respond to the change in pressure. Our mathematical model has the potential to describe these situations as well.

The erosion flux serves to limit the growth of the cake layer, i.e., the thicker it gets, the larger will be the erosion flux. Therefore, there will always be a finite cake layer thickness, not growing indefinitely. The erosion flux also depends on the transmembrane water flow rate, J_w, because the higher J_w, the more it is the case that particles are pushed on one another, i.e., the stronger, the more resilient, will be the structure, better able to withstand a certain shear force.

How to derive an expression for the erosion flux, $J_{erosion}$, that depends on water flow rate and on cake layer thickness? The following approach leads to a simple but insightful expression for $J_{erosion}$. We define coordinate x to start at the membrane surface, directed towards the top of the cake layer, which is located at $x = \delta$, i.e., δ is the cake layer thickness. The model is based on the following approach. At each position in the layer particles (droplets) are 'jammed' into place, i.e., they are more or less strongly 'locked' in place between upper and lower layers. Also the more strongly they are locked in place, the less likely will it be for an 'erosion event' to occur, for droplets to make a certain shift in position along one another, similar to layers sliding past one another. This moment of force is proportional the force by which all upper layers push on a certain layer of particles [29]. Here 'upper' refers to all material (droplets) between position x and position δ. The water flowing through the layer pulls on each 'differential layer', dx, by a force that is proportional to J_w and is inversely proportional to the cake layer permeability, k. This is Darcy's law. Thus the force acting on the particles at position x equals the pressure drop over the layer on top, due to water flow, i.e.,

$$\text{lock} - \text{inforce} \propto J_w(\delta - x)/k. \tag{7}$$

The next step is to assume that the likelihood, or frequency, of an 'erosion event', a stochastic process, depends by an exponential power on the sum of forces that act on a layer of particles or droplets. One contribution is the shear force that is applied to the cake layer. The fluid that passes the cake layer drags on it by a force that is counteracted by shear stresses that develop inside the cake layer. For a planar cake layer, this stress that is exerted in a direction parallel to the membrane, τ, is independent of depth x, i.e., at each position in the layer the particles are subjected to the same stress, in the direction along the membrane. It is not the case that deeper layers are cushioned somehow from this effect. This statement is the result of a force balance on an elastic layer that is clamped (fixed in space) on one end, and subjected to a shear force on the other end: the stresses in the layer are everywhere the same, independent of depth. The shear stress τ is what drives the erosion process. This tendency to erode can be reduced by the earlier-described moments of force or lock-in effect. These two effects are now combined into an expression for the frequency of an erosion event, which we describe by

$$\mathscr{F} = \exp(\tau - \alpha \cdot (\delta - x)J_w) \tag{8}$$

where we introduce a factor α, which is inversely proportional to permeability k, multiplied by an unknown factor to translate from force to an 'transition energy' for an erosion event to occur. A similar prefactor could also be placed in front of τ and another one in front of the entire exp-term, but they will ultimately be combined with the unknown τ anyway, so there is no need to add them at this stage.

Thus, the above equation predicts the likelihood of an erosion event at a certain position x. We can assume that the total erosion at that position in the layer, i.e., the relative movement of material past one another, is proportional to this likelihood. And we can assume that the erosion of the full layer, is then given by this term, integrated over the full layer thickness. One then arrives at

$$J_{erosion} = \int_0^\delta \mathscr{F}\,dx = \frac{\beta}{\alpha J_w}(1 - \exp(-\alpha\delta J_w)) \tag{9}$$

where $\beta = \exp(-\tau)$. Additional prefactors could have been implemented in the transformation from likelihood to total erosion flux but these factors all simply end up in β.

For low thickness or low water flow rates, the expression for erosion flux simplifies to

$$J_{erosion} = \beta\delta \tag{10}$$

irrespective of water flow rate. In this limit, there simply is no 'stabilization' at all, and the erosion likelihood is $\exp(\tau)$, equal at all positions in the (thin) layer. Thus, the 'amount of' erosion scales linearly with layer thickness. In any calculation, even at high τ, with this expression for $J_{erosion}$, the theory predicts there always is a cake layer, with at least a fleetingly small thickness. The other limit is that of a thick layer or large water flow rate, and in that case the erosion flux levels off at $J_{erosion} = \beta/(\alpha J_w)$, i.e., now the erosion flux has become independent of thickness and only depends on the water flow rate. In this case, inner layers are so strongly pushed on one another, the likelihood of an erosion event deep in the layer

is vanishingly small, and erosion events can only occur in the top of the cake layer, and the more of them, thus more erosion, at low values of the stabilizing force, which is the transmembrane water flow. Because this water flow decreases when the layer grows, the theory will lead to a finite steady-state layer thickness.

This finalizes our explanation of the new expression for J_{erosion} which can be used in the full model for the dynamics of cake layer growth, Eq. (6). Note that our calculations make use of the full numerical equation for J_{erosion} of Eq. (9), and we do not use any of the simplifications just discussed. However, for the experimental condition modeled, our results were independent of α (see table S1, SI) and therefore it can be inferred that the simplified equation forJ_{erosion}, i.e. Eq. (10) would suffice.

2.2. Model implementation

In this section an explanation is given on how to use and apply the attached spreadsheet model to describe and gain a better understanding of experimental data collected for crossflow filtration of O/W emulsions. For this, it is important that the experimental data are of high quality, and that flux of water through the membrane, J_w, is given as a function of permeate volume. Moreover, the applied pressure, ΔP, oil content in both feed and permeate, oil-membrane contact angle in surfactant aqueous solution, CA, and feed emulsion properties, such as droplet size, D_p, and viscosity, μ, need to be measured and provided. We first discuss the measured experimental parameters essential as input to the model calculations, while subsequently we discuss the four fitting parameters that were used to obtain a better understanding of the previously discussed fouling mechanisms. A flowchart reported in Supplementary Material, Fig. S1, summarizes the steps followed in the implementation and validation of this quantitative model.

The measured process and physical parameters from experimental data used to numerically solve Eq. (6), and therefore calculate the cake layer thickness δ (m), are the applied pressure ΔP (Pa), the membrane surface area A_{memb} (m^2), the feed viscosity μ (Pa·s), the average diameter of the oil droplets D_p (5 μm [1,2]), and the oil volume fraction in the retentate, $\phi_\infty - \phi_{perm}$, ratio between oil retention (from our previous work [1,2]) and density. The experimental parameters that are measured for the calculation of the membrane resistance due to pore blocking R_m (m^{-1}) via Eq. (3) are the oil-membrane contact angle CA (°), reported in Table S1 (SI), and the resistance of the clean membrane R_0 (m^{-1}). In all cases the permeate volume v (L) is variable.

On the other hand, some parameters need to be assumed in order to fit the experimental data. To calculate the membrane resistance due to pore blocking R_m (m^{-1}) the only fitting parameter is τ_{pb} (Eq. (3)), which accounts for how fast droplets adhere and block (spread over) the membrane pores. To calculate the cake layer thickness δ (m), three parameters need to be fitted. One is the volume fraction of oil in the cake layer ϕ_{cl}, while the other two are used to calculate the cake erosion flux $J_{erosion}$, and they are α and β (see Eq. (6) and (9)).

3. Results and discussion

In this section we compare our model predictions with experimental data from our previous work [1,2]. We show how our model, described in the previous section, allows for quantitative prediction of membrane fouling as a function of membrane type, surfactant type and feed salinity, and provides an excellent description of the experimental data. The results of our model offer to the reader the opportunity to link quantitatively the main fouling phenomena during filtration of oily wastewater (i.e. pore blocking and cake layer) to experimental evidence of such phenomena for MF/UF systems. The results of this section open up new pathways for membrane fouling understanding, prevention and control.

3.1. Effect of membrane type

The type of membrane used during filtration will be quite important in its fouling behaviour. Membrane surface chemistry, roughness, pore size, and charge can all influence the interaction with and retention of oil droplets and thereby fouling [12]. In this work, we modeled the fouling behaviour for two different types of membrane. One is a commercially applied ceramic membrane based on silicon carbide (SiC) [2].The other one is a regenerated cellulose (RC) membrane [30,1].

Fig. 2 shows the flux decline for SiC and RC membranes during crossflow filtration of CTAB-stabilized O/W emulsions with 1 mM NaCl as background salt. Further details on the experimental conditions are reported in our previous work [1,2], while the model parameters used are reported in Table S1 of SI. The results are expressed in terms of normalized flux as a function of permeate volume per unit of membrane area (L/m^2).

Fig. 2A shows that indeed surface chemistry plays a crucial role in membrane fouling, as the RC membrane reports a lower flux decline compared to the SiC membrane. While we do observe only a ∼20% flux decline for the RC membrane, fouling is more severe for the SiC membrane with ∼50% flux decline. The model describes the experimental data very well, and can provide us with insights that we cannot simply obtain from pure experimental data, i.e. by only looking at the reported flux decline curves of Fig. 2A. Fig. 2B shows the trend of cake layer thickness and areas of the pores blocked (due to pore blocking) by the oil as a function of permeate volume. Pore blocking is the main mechanism responsible for the flux decline, with up to ∼50% of blocked area for SiC membrane and only ∼20% for the RC membrane. This is in line in with the values that we observed from the flux decline curves, as the decrease in flux is proportional to the area of the membrane where the pores are blocked. Additionally, our model points out that pore blocking occurs faster for SiC than for the RC membrane. For both membranes the cake layer remains thin and does not constitute the main resistance to the water flux. However, we can see that the cake layer thickness is higher for SiC than for the RC membrane, in agreement with the higher crossflow velocity applied in the experiments with the RC membrane. A higher crossflow velocity translates into a higher erosion flux which decreases the thickness of the cake layer. Another reason behind the higher cake layer thickness for SiC can be found in the higher water permeability, and therefore drag force acting on the oil droplets and pushing them to the membrane interface. Overall our model thus confirms that the different fouling behaviour of two membranes with different surface chemistries (but identical emulsions), can be well explained by the way that the oil droplets spread over the membranes surface. SiC has a high negative surface charge, while the emulsion was stabilized by cationic surfactant, likely leading to a lower contact angle compared to the lesser charged RC membrane (Table B1, Appendix B).

3.2. Effect of surfactant type

Surfactants have strong effects on membrane fouling by oily-wastewater, as these molecules adsorb at the oil–water and membrane-water interface, influencing the mutual interaction between the droplets in the fouling layer as well the membrane surface chemistry [1,8,31,32].

Fig. 3 shows the effect of surfactant chemistry on flux decline during crossflow filtration with the SiC membrane of surfactant-stabilized O/W emulsions. Anionic SDS, cationic CTAB, zwitterionic

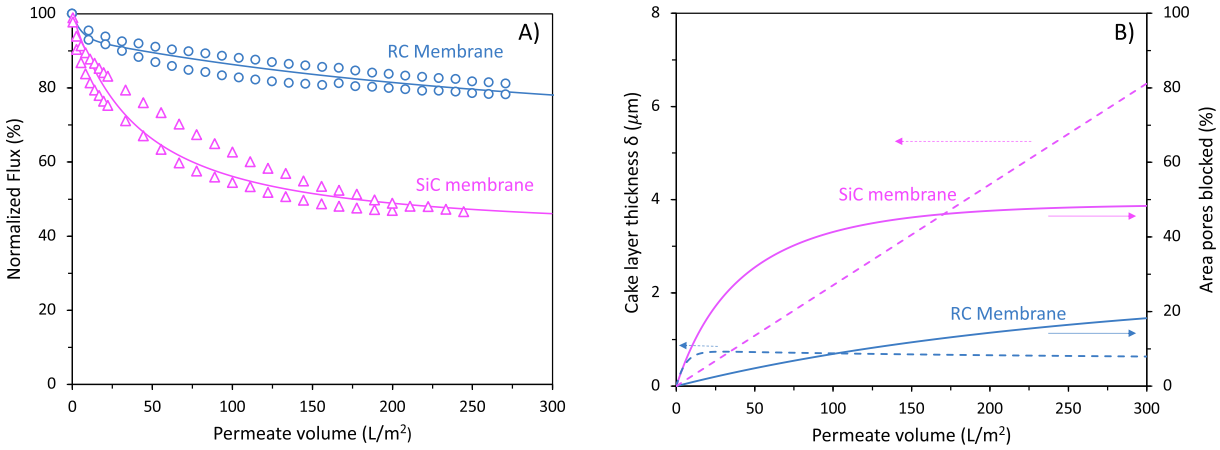

Fig. 2. A) Flux decline and B) cake layer thickness, δ, and Area of blocked pores (%), for CTAB (~350 mg/L, 1 mM NaCl) stabilized emulsions for SiC and regenerated cellulose (RC) membranes. For SiC membrane: pore size = 150 nm, water flux = 300 $Lm^{-2}h^{-1}$, crossflow velocity = 7.6 cm/s, TMP = 0.1 bar. For RC membrane: pore size = 40–80 nm, water flux = 200 $Lm^{-2}h^{-1}$, crossflow velocity = 20 cm/s, TMP = 1 bar. Symbols represent data points from our previous experiments [1,2], while lines are generated by the present model. All the experiments were performed in duplicate, as shown.

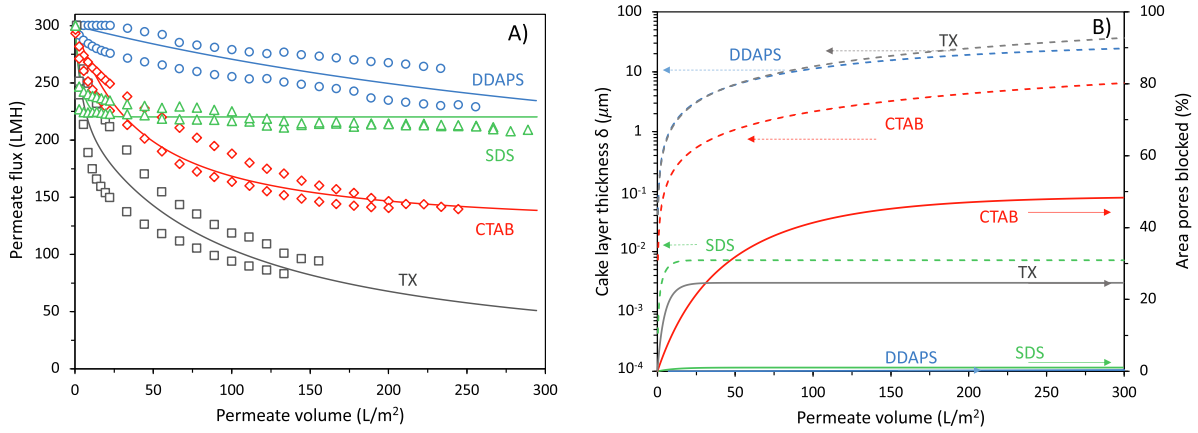

Fig. 3. A) Flux decline and B) cake layer thickness, δ, and Area of blocked pores (%), for stabilized emulsions filtered by a SiC membrane as a function of surfactant type for SDS (~2400 mg/L), CTAB (~350 mg/L), DDAPS (~1000 mg/L) and TX (~150 mg/L) in presence of 1 mM NaCl. Pore size = 150 nm, water flux = 300 $Lm^{-2}h^{-1}$, crossflow velocity = 7.6 cm/s, TMP = 0.1 bar. Symbols represent data points from our previous experiments [2], while lines are generated by the present model. All the experiments were performed in duplicate, as shown.

DDAPS, and nonionic TX were used to stabilize the emulsions. All the experiments here reported were performed at low salinity (1 mM NaCl) to better show the effect of surfactant chemistry on flux decline. In Fig. 3A we can observe that nonionic TX fouls the most, while the zwitterionic DDAPS fouls the least. The cationic CTAB fouls more than SDS, in agreement with their respective charges compared to that of anionic membrane.

Again the model successfully describes the flux decline curves. Moreover, it provides us with interesting results that can help us to better understand the specific fouling mechanisms and reasons hidden behind the observed flux decline. Fig. 3B shows that while for the cationic CTAB pore blocking is the dominating mechanism, with a ~50% of pores blocked area, the situation with the anionic is that a rather dense oil layer prevails (~0.93, table S1, SI). On the other hand, while for DDAPS we do not observe any pore blocking, in line with the known antifouling property of zwitterions, we do observe a relatively thick (~25μm) cake layer, although with a low resistance and thus a very limited effect on the flux. For TX both fouling mechanisms are quite strong, with around 25% blocked area and highest cake layer thickness ~35μm. Additionally, it is noted that for TX the layer is quite dense. Without charges the oil droplets are unlikely to be as well stabilized by TX as by the other surfactants and this leads to a denser cake layer and possibly to increased droplet coalescence.

Finally, we can attribute the higher thickness of the cake layer obtained for TX and DDAPS O/W emulsion to the lower erosion flux (see table S1), which is in line with the neutral net charge of these surfactants. It is expected that if surfactants are not charged, the repulsive forces between the surfactants and therefore the droplets are way lower than for charged surfactants. This makes the cake layer more resistant and more difficult to erode, compared to a CTAB or SDS stabilized cake layer where repulsive forces between the droplets dominate as a consequence of the fact that surfactant of same charge (positive or negative) are stabilizing the oil droplets.

Our model describes elegantly how the fouling mechanisms can change when the emulsion droplets are stabilized by different surfactant types.

3.3. *Effect of salinity*

Salinity is know to have substantial effects on oil droplets stability and membrane fouling, especially in the case of charged surfactants [1,8,12,33]. Fig. 4 shows the effect of salinity on both SiC

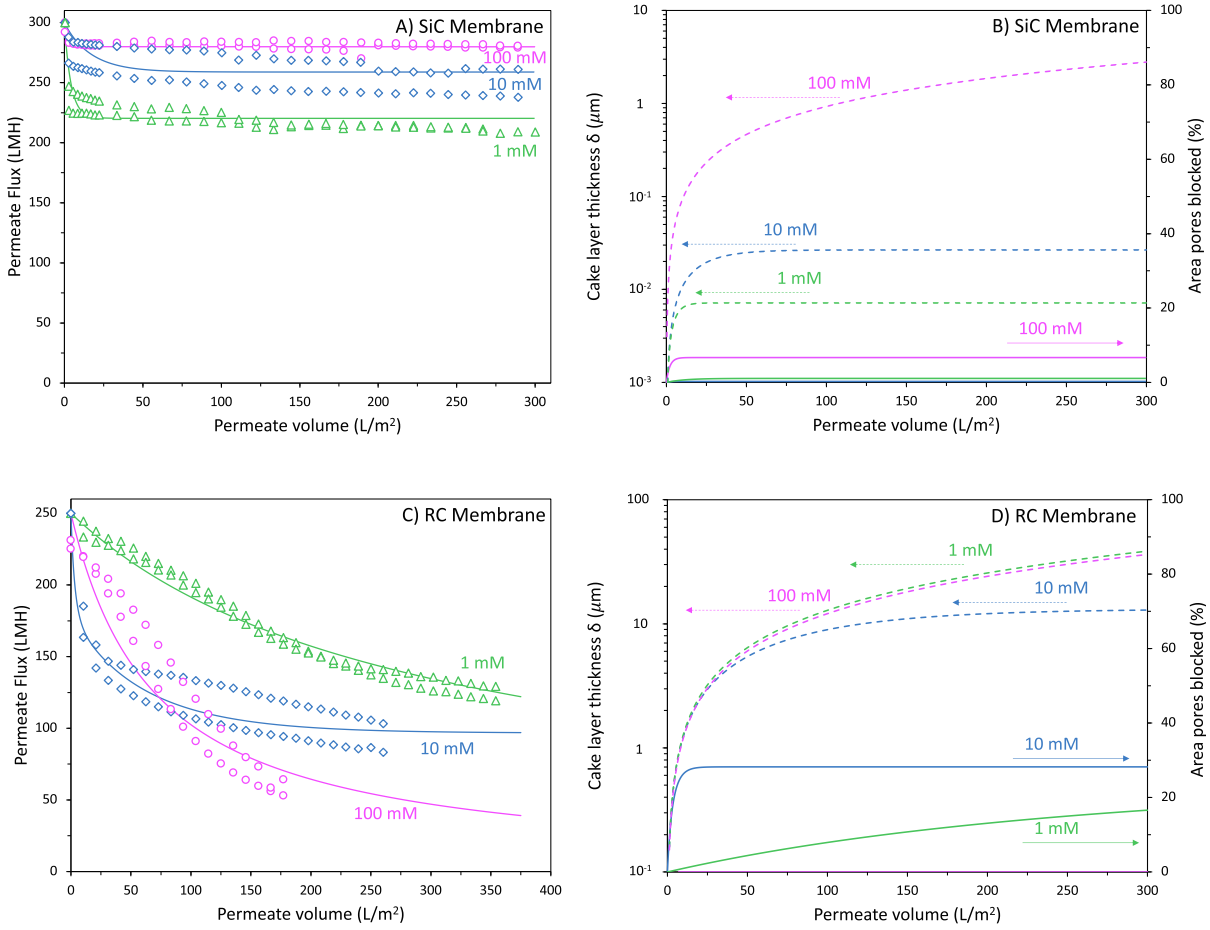

Fig. 4. Flux decline and cake layer thickness, δ, and Area of blocked pores (%), respectively, of SDS stabilized emulsions for A) B) SiC and C) D) regenerated cellulose (RC) membranes as a function of salinity (1, 10 and 100 mM NaCl). A) and B): pore size = 150 nm, water flux = 300 $Lm^{-2}h^{-1}$, crossflow velocity = 7.6 cm/s, TMP = 0.1 bar, and ~2400 mg/L SDS. C) and D): pore size = 40–80 nm, water flux = 200 $Lm^{-2}h^{-1}$, crossflow velocity = 20 cm/s, TMP = 1 bar, and ~460 mg/L SDS. Symbols represent data points from our previous experiments [1,2], while lines are generated by the present model. All the experiments were performed in duplicate, as shown.

and RC membranes for anionic SDS based emulsions. While in the case of SiC an increase in salinity translates into reduced fouling, for the RC membrane it is the opposite. Here the model gives us insights on such behavior.

The main reason for a lower flux decline observed for the SiC membrane can be attributed to a reduced build-up of oil on the SiC membrane surface [2], where the oil does not block the membrane pores or lead to the formation of a cake layer. On the other hand, the oil is mainly retained by the RC membrane, and therefore we do observe both pore blocking and cake layer mechanisms. This difference in the build-up of oil on the membrane surface is mainly due to the fact that the SiC membrane was tested at higher concentrations of SDS (2390 mg/L) than RC membrane (460 mg/L), which translates into higher droplet deformability and therefore increased oil passage.

For the SiC membrane filtrating SDS stabilized emulsions, higher ionic strengths translate into lower decline of the water flux through the membrane. At higher salinity, the interfacial tension of the droplets becomes even lower further increasing oil permeation and thus reducing the build-up of oil on the membrane surface.

For the RC membrane, where the oil is retained a thicker cake layer is observed for all ionic strengths (~13–40μm), and some pore blocking is observed, ~20% of blocked pores area for 1 mM, which then increases to ~30% for 10 mM, to finally fall to zero for 100 mM. However, it is the cake layer resistance that dominates as the porosity is low. Moreover, the density of the cake layer increases with salinity, again suggesting the presence of a rather dense oil cake layer on top of the membrane. At a higher salinity the charge repulsion between the emulsion droplets will be smaller, allowing a smaller distance between the droplets, moreover coalescence also become much more likely.

To conclude, the model can also provide a good description for for the complex effects on membrane fouling at different salinities. Higher oil permeation with increasing salinity reduces the amount of oil that can foul the membranes as observed for the SiC membrane. For the RC membrane where the oil is well retained the density of the cake layer becomes the key in understanding the increasing fouling at higher salinities, where a reduction in charge repulsion between droplets generates a more compact cake layer.

4. Conclusions

While previous studies [18–22] have investigated and tried to model fouling for MF and UF membranes by using Hermia's fouling model [16], in this work, we have presented and validated a new quantitative fouling model able to describe cake layer formation and pore blocking for membrane fouling of porous membranes during PW treatment, giving for the first time specific insights on the fouling mechanisms based on measurable emulsion (feed)

properties (e.g. oil droplet size, oil permeation, oil-membrane contact angle, etc.).

While Hermia's model has been an excellent phenomenological model, it is only a qualitative tool as it does not predict fouling a priori but it is limited by being based on pure fitting as is the recent approach of Wu [23]. Moreover, an underlying assumption is that the fouling agents act as solids, while emulsion droplets are well known to be able to deform and coalesce. Here, our model offers clear advances in one of the complex fields of colloid and interface science, membrane fouling. Our model is used to describe experimental data of previous works [1,2] where membrane type, surfactant type and salinity of the feed stream were varied. Most input parameters can be taken directly from the experimental conditions, and just four fitting parameters are required. In our model the degree of pore blocking is determined by the membrane contact angle and the resulting surface coverage, while the cake layer is described by a mass balance and a cake erosion flux.

Overall our model confirms that the different fouling behaviour of two membranes with different surface chemistries (but identical emulsions), can be well explained by the way that the oil droplets spread over the membranes surface thereby blocking the membrane pores. Our model also describes in a elegant way how the fouling mechanisms can change when the emulsion droplets are stabilized by different surfactant types, and can provide a good description of the complex effects on membrane fouling at different salinities. Higher oil permeation with increasing salinity reduces the amount of oil that can foul the membranes as observed for the SiC membrane. For the RC membrane where the oil is well retained the density of the cake layer becomes a predominant factor in understanding the increasing fouling at higher salinities, where a reduction in charge repulsion between droplets generates a more compact cake layer. In addition, this model is not limited to SiC and RC membranes but it can be successfully applied to predict fouling by different O/W emulsions for other MF and UF membrane materials when the oil droplets are much larger than the membrane pores. These results, and the model developed therefrom, opens up new pathways for understanding membrane fouling, its prevention and control.

CRediT authorship contribution statement

Ettore Virga: Conceptualization, Methodology, Validation, Investigation, Resources, Data curation, Writing – original draft, Visualization, Supervision, Project administration. **Robert W. Field:** Validation, Resources, Writing – review & editing. **P.M. Biesheuvel:** Conceptualization, Writing – review & editing, Supervision, Visualization, Funding acquisition. **Wiebe M. de Vos:** Conceptualization, Writing – review & editing, Visualization, Supervision, Funding acquisition.

Declaration of Competing Interest

The authors declare that they have no known competing financial interests or personal relationships that could have appeared to influence the work reported in this paper.

Acknowledgement

This work was performed in the cooperation framework of Wetsus, European Centre of Excellence for Sustainable Water Technology (www.wetsus.nl). Wetsus is co-funded by the Dutch Ministry of Economic Affairs and Ministry of Infrastructure and Environment, the European Union Regional Development Fund, the Province of Fryslân and the Northern Netherlands Provinces. This work is part of a project that has received funding from the European Union's Horizon 2020 research and innovation programme under the Marie Skłodowska-Curie grant agreement No 665874. The authors thank the participants of the research theme "Desalination & Concentrates" for fruitful discussions and financial support.

Appendix A. Supplementary material

Supplementary data associated with this article can be found, in the online version, at https://doi.org/10.1016/j.jcis.2022.04.039.

References

[1] J.M. Dickhout, E. Virga, R.G. Lammertink, W.M. de Vos, Surfactant specific ionic strength effects on membrane fouling during produced water treatment, J. Colloid Interface Sci. 556 (2019) 12–23.
[2] E. Virga, B. Bos, P.M. Biesheuvel, A. Nijmeijer, W.M. de Vos, Surfactant-dependent critical interfacial tension in silicon carbide membranes for produced water treatment, J. Colloid Interface Sci. 571 (2020) 222–231.
[3] M.A. Al-Ghouti, M.A. Al-Kaabi, M.Y. Ashfaq, D.A. Da'na, Produced water characteristics, treatment and reuse: A review, J. Water Process Eng. 28 (2019) 222–239.
[4] A. Echchelh, T. Hess, R. Sakrabani, Reusing oil and gas produced water for irrigation of food crops in drylands, Agric. Water Manag. 206 (2018) 124–134.
[5] M. Wenzlick, N. Siefert, Techno-economic analysis of converting oil & gas produced water into valuable resources, Desalination 481 (2020) 114381.
[6] E. Tummons, Q. Han, H.J. Tanudjaja, C.A. Hejase, J.W. Chew, V.V. Tarabara, Membrane fouling by emulsified oil: A review, Sep. Purif. Technol. 248 (2020) 116919.
[7] B. Chakrabarty, A. Ghoshal, M. Purkait, Ultrafiltration of stable oil-in-water emulsion by polysulfone membrane, J. Membr. Sci. 325 (2008) 427–437.
[8] J. Dickhout, J. Moreno, P.M. Biesheuvel, L. Boels, R. Lammertink, W.M. de Vos, Produced water treatment by membranes: A review from a colloidal perspective, J. Colloid Interface Sci. 487 (2017) 523–534.
[9] M. Ebrahimi, K.S. Ashaghi, L. Engel, D. Willershausen, P. Mund, P. Bolduan, P. Czermak, Characterization and application of different ceramic membranes for the oil-field produced water treatment, Desalination 245 (2009) 533–540. Engineering with Membranes 2008.
[10] M. Ebrahimi, D. Willershausen, K.S. Ashaghi, L. Engel, L. Placido, P. Mund, P. Bolduan, P. Czermak, Investigations on the use of different ceramic membranes for efficient oil-field produced water treatment, Desalination 250 (2010) 991–996.
[11] A.H. Behroozi, M.R. Ataabadi, Improvement in microfiltration process of oily wastewater: A comprehensive review over two decades, J. Environ. Chem. Eng. 9 (2021) 104981.
[12] S. Huang, R.H. Ras, X. Tian, Antifouling membranes for oily wastewater treatment: Interplay between wetting and membrane fouling, Current Opin. Colloid Interface Sci. 36 (2018) 90–109. Wetting and Spreading.
[13] A. Ullah, H.J. Tanudjaja, M. Ouda, S.W. Hasan, J.W. Chew, Membrane fouling mitigation techniques for oily wastewater: A short review, J. Water Process Eng. 43 (2021) 102293.
[14] R. Field, S. Hang, T. Arnot, The influence of surfactant on water flux through microfiltration membranes, J. Membr. Sci. 86 (1994) 291–304.
[15] R.S. Faibish, Y. Cohen, Fouling and rejection behavior of ceramic and polymer-modified ceramic membranes for ultrafiltration of oil-in-water emulsions and microemulsions, Colloids Surf., A 191 (2001) 27–40.
[16] J. Hermia, Constant Pressure Blocking Filtration Law Application to Powder-Law Non-Newtonian Fluid, Trans. Inst. Chem. Eng. 60 (1982) 183–187.
[17] R. Field, D. Wu, J. Howell, B. Gupta, Critical flux concept for microfiltration fouling, J. Membr. Sci. 100 (1995) 259–272.
[18] A. Koltuniewicz, R. Field, T. Arnot, Cross-flow and dead-end microfiltration of oily-water emulsion. Part I: Experimental study and analysis of flux decline, J. Membrane Sci. 102 (1995) 193–207.
[19] Y. Pan, W. Wang, T. Wang, P. Yao, Fabrication of carbon membrane and microfiltration of oil-in-water emulsion: An investigation on fouling mechanisms, Sep. Purif. Technol. 57 (2007) 388–393.
[20] A. Salahi, M. Abbasi, T. Mohammadi, Permeate flux decline during UF of oily wastewater: Experimental and modeling, Desalination 251 (2010) 153–160.
[21] M. Abbasi, M.R. Sebzari, A. Salahi, B. Mirza, Modeling of membrane fouling and flux decline in microfiltration of oily wastewater using ceramic membranes, Chem. Eng. Commun. 199 (2012) 78–93.
[22] K. Masoudnia, A. Raisi, A. Aroujalian, M. Fathizadeh, Treatment of Oily Wastewaters Using the Microfiltration Process: Effect of Operating Parameters and Membrane Fouling Study, Sep. Sci. Technol. 48 (2013) 1544–1555.
[23] J. Wu, Improving Membrane Filtration Performance Through Time Series Analysis. (2021) 1–7
[24] A. Salama, Modeling of flux decline behavior during the filtration of oily-water systems using porous membranes: Effect of pinning of nonpermeating oil droplets, Sep. Purif. Technol. 207 (2018) 240–254.
[25] H.J. Tanudjaja, J.W. Chew, Assessment of oil fouling by oil-membrane interaction energy analysis, J. Membr. Sci. 560 (2018) 21–29.

[26] M. Galvagno, G.Z. Ramon, Hydrodynamic-Colloidal Interactions of an Oil Droplet and a Membrane Surface, Langmuir 36 (2020) 2858–2864. PMID: 32101009.
[27] T. Darvishzadeh, B. Bhattarai, N.V. Priezjev, The critical pressure for microfiltration of oil-in-water emulsions using slotted-pore membranes, J. Membr. Sci. 563 (2018) 610–616.
[28] R.W. Field, J.J. Wu, Modelling of permeability loss in membrane filtration: Re-examination of fundamental fouling equations and their link to critical flux, Desalination 283 (2011) 68–74. Special issue in honour of Professor Tony Fane on his 70th Birthday.
[29] S. Kuiper, C. van Rijn, W. Nijdam, G. Krijnen, M. Elwenspoek, Determination of particle-release conditions in microfiltration: a simple single-particle model tested on a model membrane, J. Membr. Sci. 180 (2000) 15–28.
[30] J.M. Dickhout, R.G.H. Lammertink, W.M. de Vos, Membrane Filtration of Anionic Surfactant Stabilized Emulsions: Effect of Ionic Strength on Fouling and Droplet Adhesion, Colloids Interfaces 3 (2019).
[31] D. Lu, T. Zhang, J. Ma, Ceramic Membrane Fouling during Ultrafiltration of Oil/Water Emulsions: Roles Played by Stabilization Surfactants of Oil Droplets, Environ. Sci. Technol. 49 (2015) 4235–4244. PMID: 25730119.
[32] T.A. Trinh, Q. Han, Y. Ma, J.W. Chew, Microfiltration of oil emulsions stabilized by different surfactants, J. Membr. Sci. 579 (2019) 199–209.
[33] E.N. Tummons, J.W. Chew, A.G. Fane, V.V. Tarabara, Ultrafiltration of saline oil-in-water emulsions stabilized by an anionic surfactant: Effect of surfactant concentration and divalent counterions, J. Membr. Sci. 537 (2017) 384–395.